Title

Small intestinal transcriptome analysis revealed changes of genes involved in nutrition metabolism and immune responses in growth retardation piglets1.

Journal

Journal of Animal Science, 97(9)

ISSN

0021-8812

Authors

Qi, Ming
Tan, Bie
Wang, Jing
et al.

Publication Date

2019-09-03

DOI

10.1093/jas/skz205

Peer reviewed

Small intestinal transcriptome analysis revealed changes of genes involved in nutrition metabolism and immune responses in growth retardation piglets[1]

Ming Qi,[*,†] Bie Tan,[*,2] Jing Wang,[*,†] Jianjun Li,[*] Simeng Liao,[*,†] Jiameng Yan,[*] Yanhong Liu,[‡] and Yulong Yin[*]

*Laboratory of Animal Nutritional Physiology and Metabolic Process, Key Laboratory of Agro-ecological Processes in Subtropical Region, National Engineering Laboratory for Pollution Control and Waste Utilization in Livestock and Poultry Production, Institute of Subtropical Agriculture, Chinese Academy of Sciences, Changsha 410125, Hunan, China; †University of Chinese Academy of Sciences, Beijing 100008, China; and ‡Department of Animal Science, University of California, Davis, CA 95616

ABSTRACT: Postnatal growth retardation (**PGR**) is common in piglets. Abnormal development in small intestine was casually implicated in impaired growth, but the exact mechanism is still implausible. The present study unveiled transcriptome profile of jejunal mucosa, the major site of nutrient absorption, in PGR and healthy piglets using RNA-sequencing (**RNA-seq**). The middle segments of jejunum and ileum, and jejunal mucosa were obtained from healthy and PGR piglets at 42 d of age. Total RNA samples extracted from jejunal mucosa of healthy and PGR piglets were submitted for RNA-seq. Lower villus height was observed in both jejunum and ileum from PGR piglets suggesting structural impairment in small intestine ($P < 0.05$). RNA-seq libraries were constructed and sequenced, and produced average 4.8×10^7 clean reads. Analysis revealed a total of 499 differently expressed genes (**DEGs**), of which 320 DEGs were downregulated in PGR piglets as compared to healthy piglets. The functional annotation based on Gene Ontology (GO) and Kyoto Encyclopedia of Genes and Genomes (KEGG) highlighted that most DEGs were involved in nutrient metabolism and immune responses. Our results further indicated decreased gene expression associated with glucose, lipid, protein, mineral, and vitamin metabolic process, detoxication ability, oxidoreductase activity, and mucosal barrier function; as well as the increased insulin resistance and inflammatory response in the jejunal mucosa of PGR piglets. These results characterized the transcriptomic profile of the jejunal mucosa in PGR piglets, and could provide valuable information with respect to better understanding the nutrition metabolism and immune responses in the small intestine of piglets.

Key words: immune response, nutrition metabolism, postnatal growth retardation, small intestine, transcriptomic analysis

J. Anim. Sci. 2019.97:3795–3808
doi: 10.1093/jas/skz205

INTRODUCTION

The small intestine plays an important role in terminal digestion and absorption of nutrients and, therefore, in postnatal growth of animals (Wu et al., 2006). However, the young pig is prone to suffering from numerous challenges and severe stress (Moeser et al., 2007). In response to these various stress, the small intestine undergoes

[1]Funding for this project from Key Programs of frontier scientific research of the Chinese Academy of Sciences (QYZDY-SSW-SMC008), National Natural Science Foundation of China (no. 31330075, 31672433, 31501964, 31560640), the Earmarked Fund for China Agriculture Research System (CARS-35), and Youth Innovation Team Project of ISA, CAS (2017QNCXTD_TBE).

[2]Corresponding author: bietan@isa.ac.cn

Received January 29, 2019.
Accepted June 19, 2019.

marked changes (Xu et al., 2000). The marked changes occurring in gut structure and function are thought to be critical for the poor performance observed (Pluske et al., 1997). It has been demonstrated that growth retardation was associated with abnormal morphology and dysfunction in intestine (Dong et al., 2014; Subramanian et al., 2014). Intrauterine growth retardation (**IUGR**) has shown a permanent stunting effect on postnatal growth and reduced the efficiency of feed/forage utilization (Wu et al., 2006). Postnatal growth retardation (**PGR**) has also been a common problem in swine production. The exact mechanisms in association with PGR are complicated and still largely unknown, but intestinal dysfunction has been widely observed that is manifested as impaired nutrient absorption capacity and deficient in mucosal immunity (Blanton et al., 2016; Charbonneau et al., 2016). Dysregulated enteric functions were ascribed to transcriptional modulation or epigenetic modulation in cases of IUGR (Ding and Cui, 2017; Hu et al., 2018). However, there is a lack of characterization on global transcriptome of intestinal mucosa in PGR piglets. RNA-sequencing has been employed as an exploratory tool to uncover transcriptional mechanism explaining mucosal functions in different parts of intestine (Wang et al., 2009; Mach et al., 2014). Therefore, comprehensive gene expression profiles in PGR and healthy piglets were analyzed using RNA-sequencing in the present study that could explore the molecular mechanism of PGR and provide new regulatory targets of intestinal function and animal growth.

MATERIALS AND METHODS

All pigs used in the current study were humanely managed according to the Chinese Guidelines for Animal Welfare. The experimental protocol was approved by the Institutional Animal Care and Use Committee of the Institute of Subtropical Agriculture, Chinese Academy of Sciences (2013020).

Animals and Experimental Design

Eight male PGR piglets (5.40 ± 0.38 kg) and 8 male healthy piglets with normal growth (11.01 ± 0.40 kg) were pair-matched by litter and enrolled in the experiment at 42 d of age. There were no obvious characteristics of the disease or injury for PGR pigs. Pigs had ad libitum access to feed and water and were housed in the same environment. They were fed same basal diets which were formulated according to the recommended nutrient requirements of National Research Council (2012) (Council, 2012). Piglets were euthanized by electrical stunning on the day of enrollment. Sections of small intestine were rinsed thoroughly with ice-cold physiological saline. The middle segments of the jejunum (2 cm) and ileum (2 cm) were cut and fixed in 4% paraformaldehyde for morphology analysis. Jejunal mucosa was scraped, snap-frozen in liquid nitrogen, and subsequently stored at −80 ℃ until total RNA extraction.

Intestinal Morphology

The jejunal and ileal morphology were determined using hematoxylin-eosin staining. Fixed tissue samples were processed following dehydration, paraffin embedding, sectioning, and staining procedures (Wang et al., 2016), images were acquired at various magnifications with computer-assisted microscopy (Micrometrics TM; Nikon ECLIPSE E200, Tokyo, Japan). Villus height, crypt depth, as well as goblet cell and lymphocyte counts (per 100 enterocytes) were measured by Image-Pro Plus software (v6.0) with 200-fold magnification in 5 randomly selected fields.

RNA Extraction and Library Preparation

The transcriptome sequencing and analysis were conducted by OE Biotech Co., Ltd (Shanghai, China). Total RNA was extracted using the mirVana miRNA Isolation Kit (Ambion, Austin, TX) following the manufacturer's protocol. RNA integrity was evaluated using the Agilent 2100 Bioanalyzer (Agilent Technologies, Santa Clara, CA). The samples with RNA integrity number (RIN) ≥ 7 were submitted for RNA-sequencing. The libraries were constructed using TruSeq Stranded mRNA LTSample Prep Kit (Illumina, San Diego, CA) according to the manufacturer's instructions. Then these libraries were sequenced on the Illumina sequencing platform (HiSeqTM 2500) and 150 bp paired-end reads were generated.

Quality Control and Reads Mapping

Raw data (raw reads) were processed using Trimmomatic (Bolger et al., 2014). The reads containing poly N and the low-quality reads were removed to obtain the clean reads. And the downstream analysis was based on the clean reads with high quality.

Reference genome and annotation files were downloaded from genome website directly. Then

the clean reads were mapped to reference Sus scrofa 11.1 genome using hisat2 (Kim et al., 2015).

Quantification and Differential Expression Analysis of Transcripts

Transcriptomic sequencing quality was displayed by mapping ratio to the reference genome and transcriptome. Based on results of clean reads mapping to reference genome, the values of fragments per kilo base of transcript sequence per millions base pairs sequenced (FPKM) of each gene were calculated using cufflinks (Trapnell et al., 2012), and the read counts of each gene were obtained by htseq-count (Anders et al., 2015). Differently expressed genes (**DEGs**) were identified using the DESeq2 (2014) (Love et al., 2014) functions estimateSizeFactors and nbinomTest. The resulting *P*-values were corrected for multiple comparison using the Benjamini and Hochberg's approach to control the false discovery rate (**FDR**). Genes with FDR < 0.05 and fold change (FC) > 2 or FC < 0.5 in comparison between PGR and healthy group were considered as differential expression. Hierarchical cluster analysis of DEGs was performed to explore genes expression pattern. Gene Ontology (**GO**) enrichment and Kyoto Encyclopedia of Genes and Genomes (**KEGG**) pathway enrichment analysis of DEGs were, respectively, performed using R based on the hypergeometric distribution. To further analyze GO/KEGG enrichments of up- or downregulated DEGs, significance of GO/KEGG enrichment score ($P < 0.05$) and number of DEGs (greater than 2) were acted as a cutoff.

Validating the Expression of DEGs by RT-qPCR

To validate the veracity and reliability of the transcriptome data, we randomly selected 12 DEGs for conducting RT-qPCR validation. Total RNA was isolated from all 16 liquid nitrogen-pulverized jejunal mucosa samples with TRIzol reagent (Takara Biotechnology Co., Ltd, Dalian, China) following the manufacturer's recommended protocol and quantified by electrophoresis on 1% agarose gel, measuring optical density (OD) at 260 and 280 nm (Wu et al., 2013). For all samples, RNA had an OD260:OD280 ratio of between 1.8 and 2.0 (Yang et al., 2016). DNA-free RNA (1 μg) was used for reverse-transcription and polymerase chain reactions. Synthesis of the first strand (cDNA) was performed with 5× PrimeScript Buffer 2 and PrimeScript reverse transcriptase Enzyme Mix 1 (Takara, Dalian, China). Primers were designed with Primer 5.0 (PREMIER Biosoft International, Palo Alto, CA) according to the gene sequence of the pig to produce an amplification product (Supplementary Material 1). Beta-actin was used as a housekeeping gene to normalize target gene transcript levels (Tan et al., 2009). The resulting cDNA was diluted and used as a PCR template to evaluate gene expression. The reaction was performed in a volume of 10 μL (LightCycler 480 Real-Time PCR System, Roche, Switzerland). One microliter cDNA template was added to a total volume of 10 μL containing 5 μL SYBR Premix Ex Taq II (Takara, Dalian, China), 3.2 μL distilled H_2O, and 0.4 μmol/L each of forward and reverse primer. Reactions were incubated in a 384-well optical plate (Roche, Switzerland). We used the following protocol: 1) predenaturation program (30 s at 95 °C), 2) amplification and quantification program, repeated 40 cycles (5 s at 95 °C and 20 s at 60 °C for annealing), and 3) melting curve program (60 to 95 °C with a heating rate of 0.1 °C per second and fluorescence measurement). All samples were tested in triplicate. The relative expression levels of the selected genes normalized against the reference gene (*β-actin*) were calculated by using the $2^{-\Delta\Delta Ct}$ method (Livak and Schmittgen, 2001). Data are expressed as the relative values to those for healthy piglets.

Statistical Analysis

Statistical analysis for intestinal morphology and relative mRNA level were performed by the independent sample *t*-test using SPSS software 20.0 (SPSS Inc., Chicago, IL). All data were presented as means ± SEM. *P*-values < 0.05 were declared for statistical significance.

RESULTS

Jejunal and Ileal Morphology

Representative hematoxylin–eosin-stained images of the jejunum and ileum are shown in Fig. 1. In the jejunum, the villus height and crypt depth in PGR piglets were shorter than that in healthy piglets ($P < 0.05$), and there were no differences in the ratio of villus height to crypt depth, goblet cell number, or lymphocyte number between 2 groups ($P > 0.05$). In the ileum, the villus height and the number of goblet cell in PGR piglets were significantly lower in comparison with healthy piglets ($P < 0.05$). No difference was observed in the crypt depth, the ratio

of villus height to crypt depth, and lymphocyte number in the ileum between the 2 groups ($P > 0.05$) (Table 1).

Quality Assessment of RNA-Sequencing

After Illumina sequencing, there were approximately 49.35 M raw reads per library. After removing and/or filtering out the adapters and low-quality tags, the average numbers of clean reads per library in healthy and PGR groups were 47.78 and 48.00 M, respectively. There were nearly same number of clean reads in 2 groups. Moreover, the percentage of GC content in all these samples was almost 50%. All the assessment criteria of base quality (Q30) were more than 92%. All data about quality of transcriptomic sequencing were shown in Supplementary Material 2.

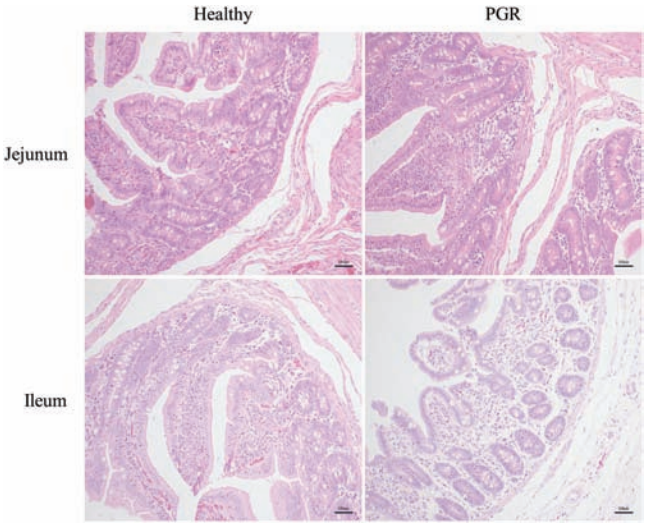

Figure 1. Representative hematoxylin–eosin-stained image (×100) of the jejunum and ileum in the healthy and PGR piglets.

Functional Annotation and Pathway Enrichment of DEGs

There were 499 DEGs (FDR < 0.05) with more than 2 FC and PGR groups were identified (Fig. 2A). Specifically, compared to the healthy group, 320 DEGs were downregulated and 179 DEGs were upregulated in PGR group. The description of total DEGs was provided in Supplementary Material 3.

The function of DEGs was annotated by GO enrichments and KEGG enrichments. Gene Ontology enrichments were divided into biological process (1,629), cellular component (234), and molecular function (518) (Fig. 2B). Top 10 total GO enrichments in each functional ontology were shown in Table 2. Pathway analysis based on KEGG database identified 244 KEGG pathways and 59 pathways were enhanced based on total DEGs ($P < 0.05$). Top 10 total KEGG pathways were shown in Table 3.

Ten top GO enrichments in each functional ontology represented by up- or downregulated DEGs (number of DEGs > 2) were shown in Figs. 3 and 4. The top enriched biological processes associated with downregulated DEGs were organic acid metabolism, epoxygenase P450 pathway, lipoprotein transport, exogenous drug catabolic process, as well as extracellular matrix (**ECM**) disassembly. The most represented cellular components involved in extracellular space, integral component of membrane, and gap junction. In the category of molecular function, arachidonic acid (**ARA**) epoxygenase activity, steroid hydroxylase activity, and metalloendopeptidase activity were enriched (Fig. 3). Upregulated DEGs primarily involved in antimicrobial humoral immune response and inflammatory response as biological process; external side of plasma membrane as cellular component;

Table 1. The jejunal and ileal morphology in the postnatal growth retardation (PGR) and healthy piglets[1]

Items	Healthy piglets	PGR piglets	*P*-value
Jejunum			
Villus height, μm	458.25 ± 20.56	363.49 ± 29.16	0.019
Crypt depth, μm	132.55 ± 4.82	105.18 ± 4.51	0.001
Villus height:crypt depth	3.49 ± 0.19	3.49 ± 0.27	0.994
Goblet cell number	7.95 ± 1.00	7.55 ± 0.70	0.748
Lymphocyte number	44.48 ± 1.77	42.73 ± 0.78	0.380
Ileum			
Villus height, μm	364.69 ± 16.70	307.07 ± 20.64	0.048
Crypt depth, μm	109.13 ± 4.28	107.30 ± 8.54	0.852
Villus height:crypt depth	3.37 ± 0.17	2.92 ± 0.21	0.119
Goblet cell number	10.55 ± 0.64	8.50 ± 0.57	0.031
Lymphocyte number	43.53 ± 1.27	44.60 ± 0.73	0.474

[1]Values are mean ± SEM; $n = 8$.

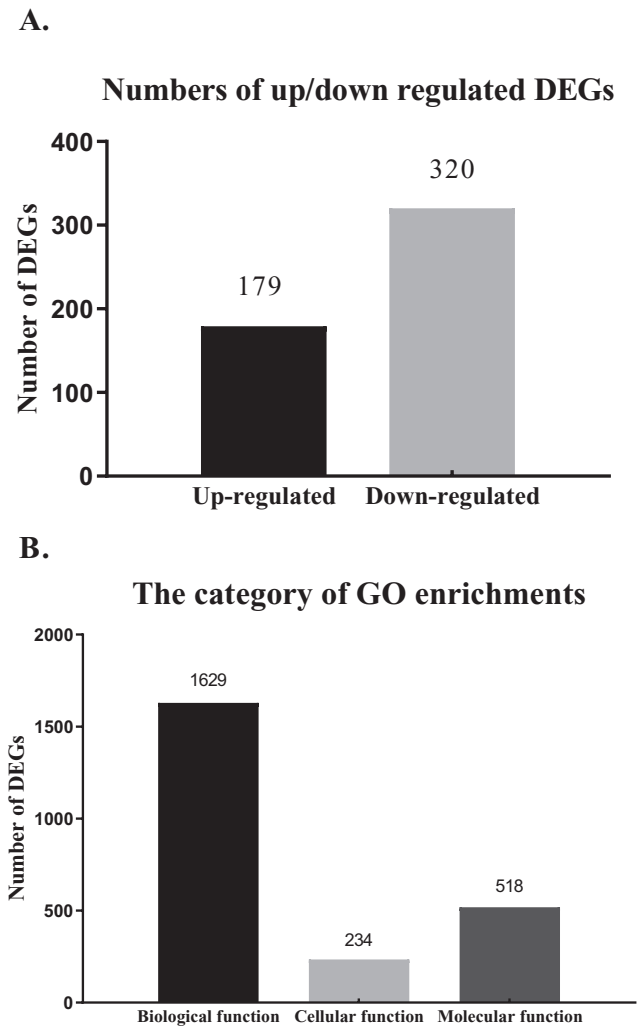

Figure 2. Clustering and category of DEGs in Illumina sequencing. (A) Numbers of up-/downregulated DEGs (n = 8). (B) The category of GO enrichments.

and symporter activity and serine-type peptidase activity as molecular function (Fig. 4).

Top 20 KEGG pathways represented by up- or downregulated DEGs (number of DEGs > 2) were shown in Figs. 5 and 6. Downregulated DEGs underscored 7 KEGG pathways related to host responses against pathogens, including ECM–receptor interaction, drug metabolism–cytochrome P450, IL-17 signaling pathway, graft-versus-host disease; while 9 pathways related to nutrient metabolism, namely retinol metabolism, mineral absorption, protein digestion and absorption, vitamin digestion and absorption (Fig. 5). While upregulated DEGs highlighted 15 pathways mainly involved in disease and inflammation response (Fig. 6).

DEGs Related to Nutrition Metabolism

Enriched GO terms associated with nutrition metabolism and corresponding DEGs were summarized in the Supplementary Material 4 (P < 0.05 and the number of DEGs annotated on GO was greater than 2). Nutrition metabolism-related GO terms include lipoprotein transport, organic acid metabolic process, zinc ion binding, calcium ion binding, glucose metabolic process, transporter activity, and cholesterol homeostasis. A total of 35 GO terms were involved with 11 being upregulated in PGR piglets (31.4%). These 11 GO terms were mainly involved in energy metabolism, nutrient transport, and signal transduction.

In addition, biosynthetic or signal transduction pathways about nutrition metabolism via KEGG annotation were significantly enriched (Supplementary Material 5). Downregulated DEGs were mapped to 19 KEGG pathways (P < 0.05, DEGs > 2 per pathway), such as vitamin digestion and absorption, PPAR signaling pathway, alanine, aspartate, and glutamate metabolism, mineral and vitamin absorption, protein digestion and absorption. Only 3 KEGG pathways enriched by upregulated DEGs were involved in nutrition metabolism including arginine biosynthesis, ARA metabolism, and pancreatic secretion.

DEGs Related to Immune Response

Enriched GO terms involved in immune response (P < 0.05, DEGs > 2 per GO term) and corresponding DEGs were listed in Supplementary Material 6. Enriched immune response terms comprise epoxygenase P450 pathway, exogenous drug catabolic process, gap junction, oxidation–reduction process, defense response to bacterium, cellular response to lipopolysaccharide, innate immune response, cytokine activity, inflammatory response, metalloendopeptidase activity, negative regulation of T-cell proliferation. These GO terms were mainly involved in chemokine, inflammatory response, signaling transduction, and cell junction, which were involved in resistance to infection.

Enriched KEGG pathways (n = 20) were associated with downregulated DEGs (P < 0.05, DEGs > 2 per pathway) involved in immune response. Examples include: ECM–receptor interaction, drug metabolism–cytochrome P450, advanced glycosylation end product-receptor of advanced glycosylation end product (AGE-RAGE) signaling pathway in diabetic complications, focal adhesion, IL-17 signaling pathway, and cytokine–cytokine receptor interaction. However, enriched pathways (n = 6) associated with upregulated DEGs were related to immune function such as insulin resistance, microRNAs in cancer, and Jak-STAT signaling pathway (Supplementary Material 7).

Table 2. Top 10 total GO enrichments in each functional ontology

ID	Term	Category	Pval	Enrichment score
GO:0032095	Regulation of response to food	Biological process	0	39.79
GO:0019373	Epoxygenase P450 pathway	Biological process	1.92E-06	23.88
GO:0006082	Organic acid metabolic process	Biological process	2.21E-06	15.92
GO:0006805	Xenobiotic metabolic process	Biological process	3.46E-06	11.05
GO:0006879	Cellular iron ion homeostasis	Biological process	3.70E-06	7.33
GO:0071421	Manganese ion transmembrane transport	Biological process	5.65E-06	19.90
GO:0019229	Regulation of vasoconstriction	Biological process	6.66E-06	13.26
GO:0001501	Skeletal system development	Biological process	1.34E-05	4.91
GO:0051281	Positive regulation of release of sequestered calcium ion into cytosol	Biological process	1.69E-05	8.65
GO:0060586	Multicellular organismal iron ion homeostasis	Biological process	2.53E-05	14.92
GO:0005615	Extracellular space	Cellular component	2.64E-11	2.68
GO:0005576	Extracellular region	Cellular component	6.34E-10	2.80
GO:0016021	Integral component of membrane	Cellular component	2.20E-06	1.42
GO:0016020	Membrane	Cellular component	5.04E-05	1.32
GO:0005922	Connexin complex	Cellular component	8.46E-05	8.38
GO:0005886	Plasma membrane	Cellular component	0.000100889	1.51
GO:0031012	Extracellular matrix	Cellular component	0.000115298	2.87
GO:0005921	Gap junction	Cellular component	0.000414189	6.12
GO:0005887	Integral component of plasma membrane	Cellular component	0.000750742	1.83
GO:0045177	Apical part of cell	Cellular component	0.000892493	3.85
GO:0005384	Manganese ion transmembrane transporter activity	Molecular function	0	39.79
GO:0020037	Heme binding	Molecular function	3.29E-07	5.84
GO:0008392	Arachidonic acid epoxygenase activity	Molecular function	1.92E-06	23.88
GO:0005506	Iron ion binding	Molecular function	4.39E-06	4.61
GO:0004181	Metallocarboxypeptidase activity	Molecular function	6.93E-06	9.95
GO:0004497	Monooxygenase activity	Molecular function	8.19E-06	6.63
GO:0016705	Oxidoreductase activity, acting on paired donors, with incorporation or reduction of molecular oxygen	Molecular function	8.19E-06	6.63
GO:0005509	Calcium ion binding	Molecular function	3.00E-05	2.21
GO:0004180	Carboxypeptidase activity	Molecular function	3.38E-05	9.95
GO:0015293	Symporter activity	Molecular function	3.62E-05	7.65

Table 3. Top 10 total KEGG pathways

ID	Term	Pval	Enrichment score
path:ssc00830	Retinol metabolism	2.14E-09	7.88
path:ssc05204	Chemical carcinogenesis	4.36E-08	6.86
path:ssc04978	Mineral absorption	5.32E-07	7.81
path:ssc05146	Amoebiasis	4.45E-06	4.55
path:ssc04974	Protein digestion and absorption	7.77E-05	3.98
path:ssc04216	Ferroptosis	9.60E-05	5.44
path:ssc00860	Porphyrin and chlorophyll metabolism	0.00015608	5.95
path:ssc05143	African trypanosomiasis	0.000186636	5.77
path:ssc00590	Arachidonic acid metabolism	0.000197173	4.30
path:ssc00250	Alanine, aspartate and glutamate metabolism	0.000307391	5.29

Validation of Expression Profiling Data by RT-qPCR

As shown in Fig. 7, PGR significantly reduced relative mRNA levels of claudin-10 (*CLDN10*), bactericidal permeability-increasing protein (*BPI*), ghrelin (*GHRL*), proto-oncogene Wnt-3 (*WNT3*), tumor necrosis factor ligand superfamily member 15 (*TNFSF15*), insulin-like growth factor-binding protein 3 (*IGFBP3*), phosphoenolpyruvate

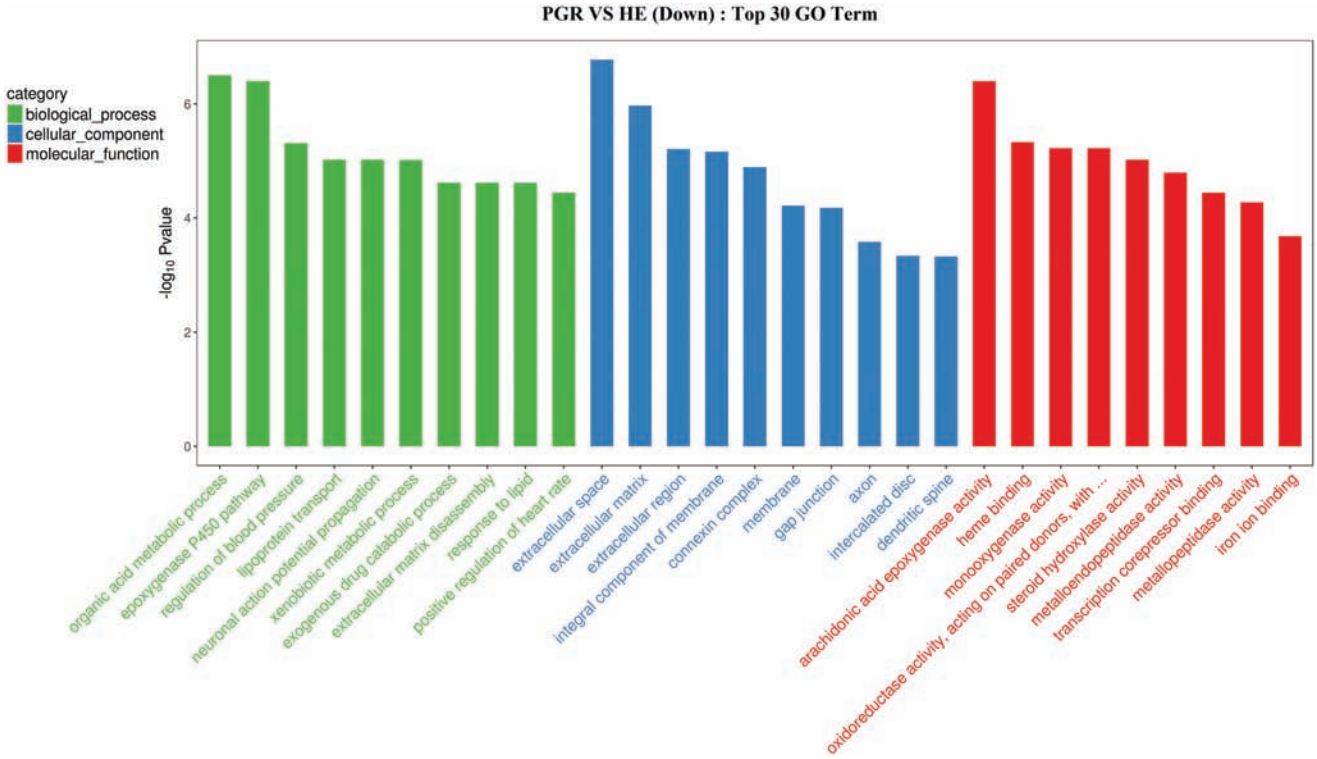

Figure 3. Top 30 GO annotation of downregulated DEGs. The numbers of DEGs in each pathway are counted and *P*-values are acquired by hypergeometric distribution test and GO enrichment scores are based on $-\log_{10}$Pvalue. Top 30 GO enrichments with downregulated DEGs larger than 2 were shown. The x-axis represents GO category terms and the y-axis represents GO enrichment scores.

carboxykinase 1 (*PCK1*), peroxisome proliferator-activated receptor gamma (*PPARγ*), matrix metallopeptidase 9 (*MMP9*), solute carrier family 39 member 4 (*SLC39A4*), cytochrome P450 C42 (*CYP2C42*), and fibronectin 1 (*FN1*) in jejunal mucosa as compared to healthy piglets ($P < 0.05$). The significantly upregulated relative mRNA expression of interleukin-6 (*IL-6*) was observed in the jejunal mucosa from PGR piglets as compared to healthy piglets ($P < 0.05$). The relative expression of 13 genes detected by RT-qPCR had the same tendency of changes with the RNA-seq, indicating the reliability of RNA-seq data.

DISCUSSION

The growth and function of small intestine are critical for optimal animal growth and health. Growth retardation is associated with abnormal intestinal morphology (Dong et al., 2014). In the present study, the PGR piglets showed decreased villus height in the jejunum and lower number of goblet cells in ileum. Impaired intestinal architecture rendered gut-associated disorders and diarrhea (Wijtten et al., 2011; McLamb et al., 2013).

This is the first study, to our knowledge, analyzing the intestinal transcriptome between the healthy and PGR piglets. A mean of 47,889,433 clean reads were obtained per library, which provide sufficient sequence coverage for transcriptional analysis. According to the results of GO and KEGG pathway analysis, the key features encoded by DEGs were related to nutrition metabolism, including PPAR signaling pathway, glucose metabolic process, mineral absorption, and protein digestion and absorption. Our findings support previous proteomics study that observed decrease of protein abundance involved in energy metabolism in the small intestinal mucosa of IUGR piglets as compared to healthy piglets (Wang et al., 2014). Peroxisome proliferator-activated receptor gamma, involved in PPAR signaling receptor pathway, is crucial to fatty acid storage, glucose metabolism, and other physiological processes (Lehrke and Lazar, 2005). The adipose-specific PPARγ knockout mice exhibited significant abnormalities in both the formation and function of brown and white adipose tissue including failing to generate adipose tissue when fed a high-fat diet (Jones et al., 2005). Intrauterine growth retardation was reported to decrease the lung and visceral fat *PPARγ* mRNA expression in neonatal rat and lamb, respectively (Duffield et al., 2009; Joss-Moore et al., 2010). In accordance with the previous results, the downregulated expression of *PPARγ* was observed in the jejunal mucosa of PGR piglets as

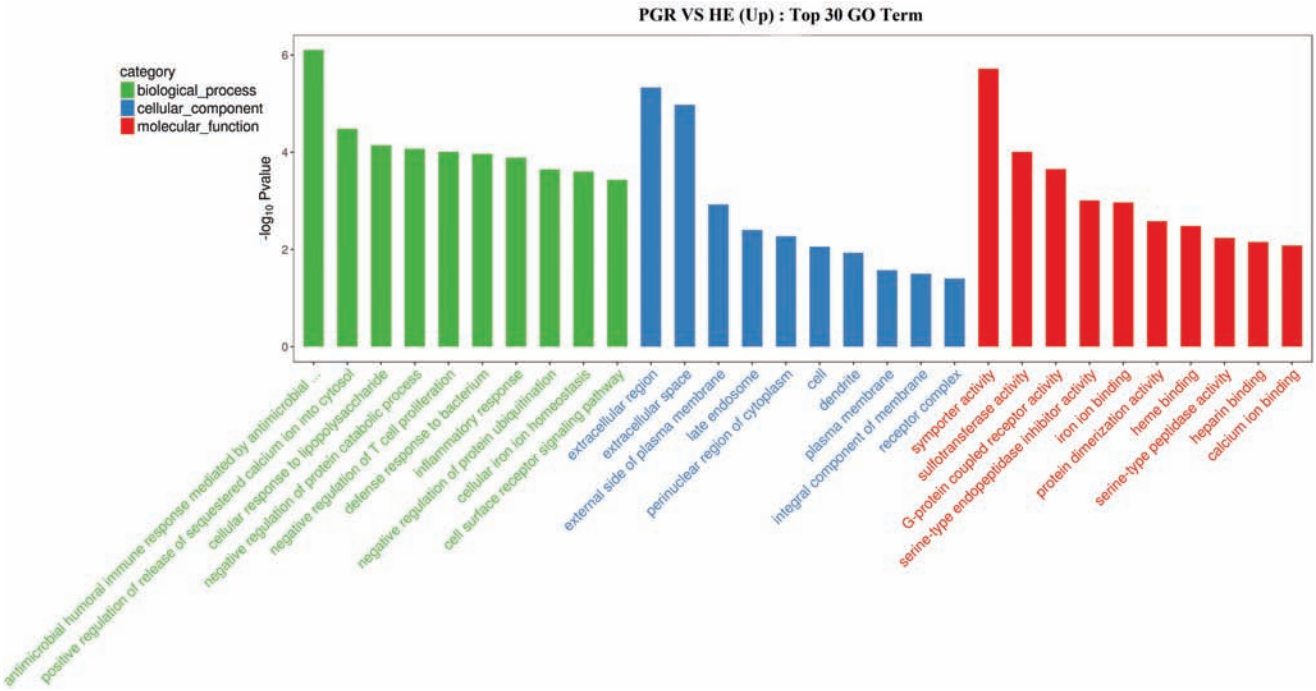

Figure 4. Top 30 GO annotation of upregulated DEGs. The numbers of DEGs in each pathway are counted and *P*-values are acquired by hypergeometric distribution test and GO enrichment scores are based on $-\log_{10}$Pvalue. Top 30 GO enrichments with upregulated DEGs larger than 2 were shown. The x-axis represents GO category terms and the y-axis represents GO enrichment scores.

compared to healthy piglets, which may be one of the factors causing lower body weight. Peroxisome proliferator-activated receptor gamma also plays an important role in insulin signaling: the loss-of-function PPARγ mutations in fat, muscle, of liver of mice and human was predisposed to developing insulin resistance (Barroso et al., 1999; Hevener et al., 2003; Matsusue et al., 2003). In our study, compared to healthy piglets, PGR induced upregulated insulin resistance involved in KEGG pathway in the jejunal mucosa. It suggests that PGR may induce an impairment in jejunal mucosal glucose utilization. Differently expressed genes involved in glucose metabolic process include phosphoenolpyruvate carboxykinase 1 (PCK1). The cytosolic enzyme encoded by *PCK1*, a rate-limiting enzyme for the regulation of gluconeogenesis, catalyzes the formation of phosphoenolpyruvate, with the release of carbon dioxide (Hanson and Patel, 1994). The downregulation of *PCK1* was reported to cause disorders of glucose and lipid metabolism in rats and compromised growth (Hanson and Patel, 1994). Intestine mucosal gluconeogenesis contributed to maintaining glucose homeostasis in the absence of hepatic glucose production (Penhoat et al., 2014). These findings were corroborated by a previous study that IUGR adult pigs exhibited damaged hepatic mitochondrial biogenesis and decreased energy metabolism (Su et al., 2017). In addition, mineral and vitamin absorption, especially retinol metabolism, associated with the ion transporter activity, was markedly decreased in jejunal mucosa of PGR piglets as compared to healthy piglets. It agreed with the previous studies that IUGR pigs showed decreased hepatic vitamins and minerals metabolism according to the hepatic proteomic analyses, and lower activity of retinol transporter in the intestinal epithelium (Wang et al., 2010; Liu et al., 2013). As retinol plays a crucial role in the adipocyte differentiation, fatty acid oxidation, and glucose transport, this may partially explain increased risk of the metabolic syndrome in the jejunal mucosa of PGR piglets. Moreover, DEGs involved in the protein digestion and absorption were downregulated in PGR piglets. This result was in accordance with the previous study that IUGR piglets were associated with a reduction in amino acid transport capacity as evidenced by the low concentration of amino acids in plasma metabolites (Lin et al., 2012). Our results highlighted reduced expression of genes encoding enzyme, transporter, and receptor, and their related pathway involved in nutrients metabolism in jejunal mucosa of PGR pigs, which might be causally linked with growth retardation.

The present study also revealed the differences in signal pathways involved in immune function, including detoxication system, oxidation–reduction process, effector molecules (e.g., cytokines), and physical barrier of jejunal mucosa. CYP450

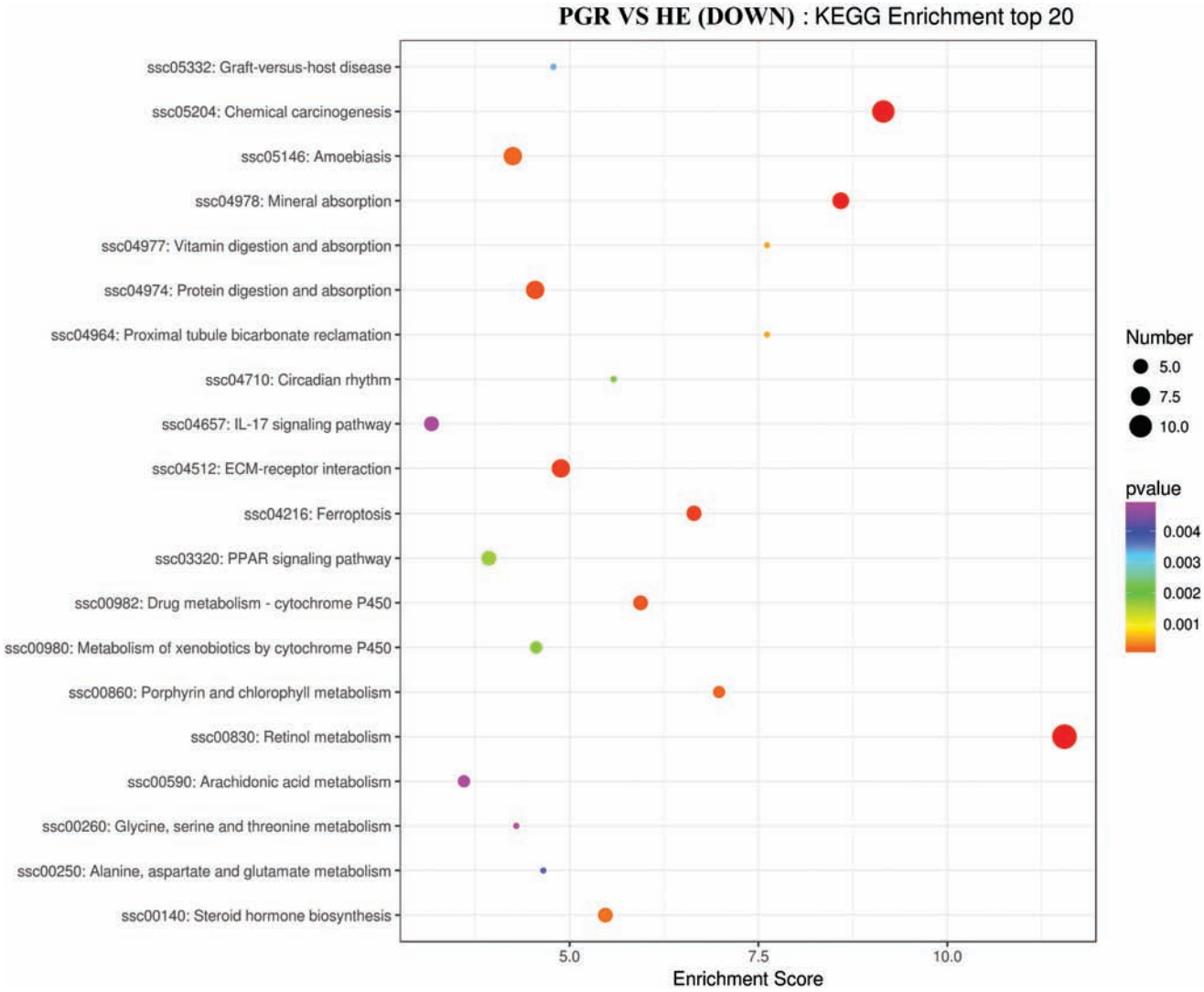

Figure 5. Top 20 KEGG annotation of downregulated DEGs. The numbers of DEGs in each pathway are counted and KEGG enrichment scores and *P*-values are acquired by hypergeometric distribution test. Top 20 KEGG enrichments with downregulated DEGs larger than 2 were shown. The x-axis represents KEGG enrichment scores and the y-axis represents pathway terms. The colors of circle indicate *P*-values and the size of circle indicates the numbers of DEGs. The circle with redder and larger indicating that the enrichment of the pathway is higher and DEG number is larger in the pathway.

enzymes, mainly expressed in digestive tract and liver, play a crucial role in the phase I biotransformation of xenobiotics (Antonissen et al., 2017). CYP450 may act as defense mechanisms against natural and synthetic environmental toxins involved in several metabolic process, such as steroid synthesis and metabolism, metabolism of ARA, and bile acid biosynthesis (Barnes, 2001; Nebert and Russell, 2002). According to the GO and KEGG analyzed results in our study, CYP450 metabolism pathway was significantly reduced in the jejunal mucosa of PGR piglets as compared to healthy piglets. It was also evidenced by the downregulated pathways involved in CYP450 metabolism in PGR piglets in our study. The low detoxication ability induced by impaired jejunal mucosa of PGR piglets may explain results. It was supported by the previous studies that IUGR may reduce hepatic drug metabolism in fetal and neonatal life of lamb evidenced by the low CYP activity in liver of lamb with low birth weight (Soo et al., 2018). CYPs also mediate oxidoreductase activity, which performs as antioxidants inside cells (Agrawal et al., 2010; Lugrin et al., 2014). Excess reactive oxygen species (ROS) can cause cellular damage and impact tissue function resulted from lipid peroxidation and DNA oxidation (Hracsko et al., 2008). Neonates with IUGR exhibited significant deficiencies in antioxidant defense, correlated with severe oxidative stress (Biri et al., 2007; Luo et al., 2018). Agreed with previous studies, our research showed PGR induced the downregulated oxidoreductase activity, which suggests that PGR piglets exhibited higher level of oxidative stress as compared to healthy piglets in the jejunal mucosa.

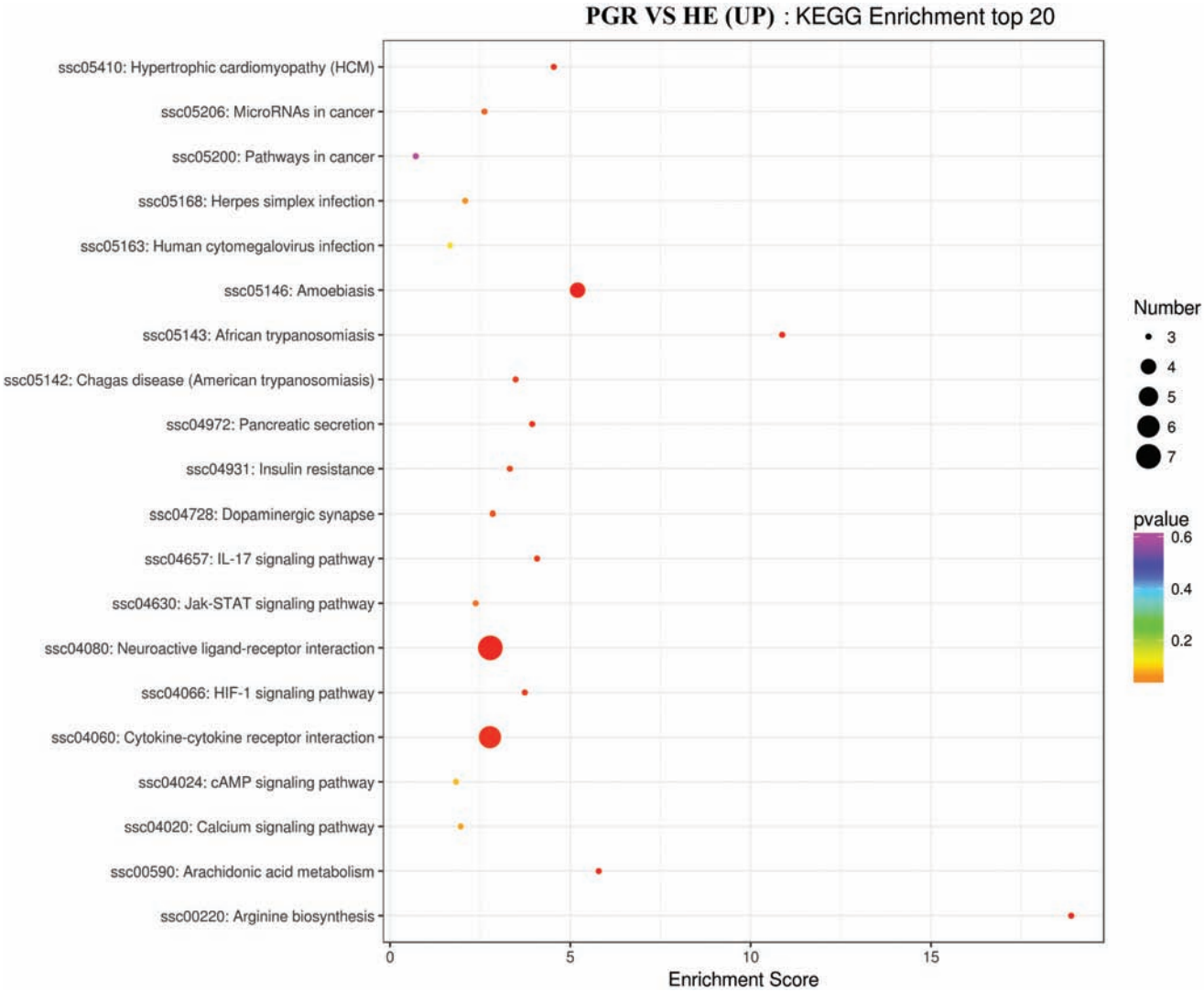

Figure 6. Top 20 KEGG annotation of upregulated DEGs. The numbers of DEGs in each pathway are counted and KEGG enrichment scores and *P*-values are acquired by hypergeometric distribution test. Top 20 KEGG enrichments with upregulated DEGs larger than 2 were shown. The x-axis represents KEGG enrichment scores and the y-axis represents pathway terms. The colors of circle indicate *P*-values and the size of circle indicates the numbers of DEGs. The circle with redder and larger indicating that the enrichment of the pathway is higher and DEG number is larger in the pathway.

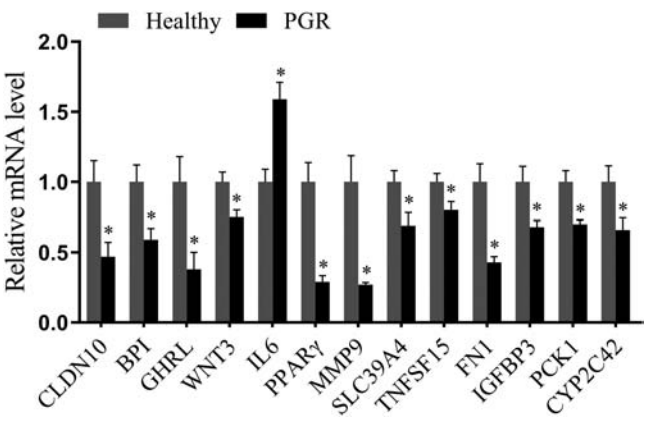

Figure 7. Relative mRNA abundances of *CLDN10*, *BPI*, *GHRL*, *WNT3*, *IL-6*, *PPARγ*, *MMP9*, *SLC39A4*, *TNFSF15*, *FN1*, *IGFBP3*, *PCK1*, and *CYP2C42* validated by RT-qPCR. Values were means ± SEM, $n = 8$. *$P < 0.05$ versus healthy piglets.

Moreover, upon binding to pathogen-associated molecular patterns (PAMPs), signaling mediated through pattern recognition receptors (PRRs) triggers innate immune responses (Jang et al., 2015). There were various DEGs involved in cytokine–cytokine receptor interaction based on KEGG annotation. *IL-1β* is strongly induced by the nuclear factor kappa B (**NF-κB**) pathway (Baggiolini and Clark-Lewis, 1992). Downregulation of *IL-1β* in PGR pigs may contribute to abnormal immune function of intestinal mucosa in PGR piglets. There are various DEGs involved in cytokine–cytokine receptor interaction in PGR piglets. The downregulated cytokines (*TNFSF15*, *IL-13*, and *IL-1β*) in the PGR piglets were previously considered as viable biomarkers of community-acquired bacterial infection

(Holub et al., 2013). This result was in consistent with the reduced gene expression of cytokines in IUGR piglet neonates (Dong et al., 2014). However, in our study, *IL-6* and *IL-17R* were upregulated in the jejunal mucosa of PGR piglets. IL-6 and IL-17, major mediators of inflammation, play pathological effects on inflammation and pathogen infection (Yen et al., 2006; Neurath and Finotto, 2011; Ren et al., 2016). It suggests that PGR may cause severe inflammation reaction in jejunal mucosa of piglets, which is evidenced by the upregulated inflammatory response annotated by GO term. It was accordance with the previous study that IUGR pigs exhibited higher expression of *IL-6* in the liver (Liu et al., 2014). Chemokine (C-C motif) ligand (CCL) and chemokine (C-X-C motif) ligand (CXCL) are 2 major subfamilies of chemokines, based on cysteine residues position (Palomino and Marti, 2015). There are 2 CC chemokines, of which *CCL20* and *CCL16* were downregulated in the jejunal mucosa of PGR piglets. In addition, CXC chemokines (*CXCL11*) were upregulated in PGR piglets. CC chemokines were reported to induce macrophage trafficking to the site of infection during *E. coli* infection (Tagawa et al., 2004). Moreover, CXC chemokines play vital roles in various bacterial infections by chemoattractants to neutrophils (Almeida Cde et al., 2009). The bicellular tight junction was downregulated in PGR piglets, which indicated that the physical barrier of jejunal mucosa in PGR piglets was impaired. The previous study also revealed that IUGR piglets induced the impairment of intestinal epithelial integrity (Zhu et al., 2017). The ECM–receptor interaction pathway plays a vital role in maintaining paracellular permeability. Our study showed the reduced expression of *FN1*, involved in ECM pathway, in the jejunal mucosa from PGR pigs. It was in consistent with the previous report that higher abundances of microRNA-29a in jejunum of IUGR pigs led to decreased levels of *FN1* (Zhu et al., 2017). Moreover, some cell junction proteins, such as *CLDN11* and *GJA5*, control cell-to-cell transmission of molecules and maintain mucosal barrier functions (Kumar and Gilula, 1996; Iwata et al., 1998). In GO annotation, the decreased cell junction and gap junction in the jejunal mucosa of PGR piglets may reveal the impaired mucosal physical barrier in PGR piglets, which agreed with the previous study that undeveloped fetal growth exhibited abnormal gap junction channel function in the placenta (Winterhager and Gellhaus, 2017). Overall, the transcriptome data have indicated that PGR has a strong impact on the mucosal barrier of jejunum in piglets.

CONCLUSIONS

Four hundred and ninety-nine DEGs were identified in the jejunal mucosa between healthy and PGR piglets. These genes may be associated with intestinal function of metabolic process and immune response. Overall, we identified key transcriptome signature of jejunal mucosa associated with PGR piglets, such as DEGs involved in nutrients metabolism, detoxication ability, and immune response. In conjunction with results of intestinal morphology, we postulated that transcriptomic modulation represents one of the molecular mechanisms that is causally linked with growth retardation.

SUPPLEMENTARY DATA

Supplementary data are available at *Journal of Animal Science* online.

Supplementary Material 1: Primer pairs used for quantitative reverse transcription-PCR.

Supplementary Material 2: RNA-seq sequencing evaluation.

Supplementary Material 3: Total differently expressed genes (DEGs) in this study.

Supplementary Material 4: DEGs related to nutrition metabolism.

Supplementary Material 5: KEGG pathway of DEGs related to nutrition metabolism.

Supplementary Material 6: DEGs related to immune response.

Supplementary Material 7: KEGG pathway of DEGs related to immune response.

ACKNOWLEDGMENTS

The authors would like to thank Changsha Lvye Biotechnology Limited Company Academician Expert Work station for the assistance in conducting the experiments.

LITERATURE CITED

Agrawal, V., J. H. Choi, K. M. Giacomini, and W. L. Miller. 2010. Substrate-specific modulation of CYP3A4 activity by genetic variants of cytochrome P450 oxidoreductase. Pharmacogenet. Genomics 20:611–618. doi:10.1097/FPC.0b013e32833e0cb5

Almeida Cde, S., C. Abramo, C. C. Alves, L. Mazzoccoli, A. P. Ferreira, and H. C. Teixeira. 2009. Anti-mycobacterial treatment reduces high plasma levels of CXC-chemokines detected in active tuberculosis by cytometric bead array. Mem. Inst. Oswaldo Cruz 104:1039–1041. doi:10.1590/s0074-02762009000700018

Anders, S., P. T. Pyl, and W. Huber. 2015. Htseq–a python framework to work with high-throughput sequencing data.

Bioinformatics 31:166–169. doi:10.1093/bioinformatics/btu638

Antonissen, G., M. Devreese, S. De Baere, A. Martel, F. Van Immerseel, and S. Croubels. 2017. Impact of Fusarium mycotoxins on hepatic and intestinal mRNA expression of cytochrome P450 enzymes and drug transporters, and on the pharmacokinetics of oral enrofloxacin in broiler chickens. Food Chem. Toxicol. 101:75–83. doi:10.1016/j.fct.2017.01.006

Baggiolini, M., and I. Clark-Lewis. 1992. Interleukin-8, a chemotactic and inflammatory cytokine. FEBS Lett. 307:97–101. doi:10.1016/0014-5793(92)80909-Z

Barnes, D. M. 2001. Expression of P-glycoprotein in the chicken. Comp. Biochem. Physiol. A. Mol. Integr. Physiol. 130:301–310. doi:10.1016/S1095-6433(01)00389-0

Barroso, I., M. Gurnell, V. E. Crowley, M. Agostini, J. W. Schwabe, M. A. Soos, G. L. Maslen, T. D. Williams, H. Lewis, A. J. Schafer, et al. 1999. Dominant negative mutations in human PPARgamma associated with severe insulin resistance, diabetes mellitus and hypertension. Nature 402:880–883. doi:10.1038/47254

Biri, A., N. Bozkurt, A. Turp, M. Kavutcu, O. Himmetoglu, and I. Durak. 2007. Role of oxidative stress in intrauterine growth restriction. Gynecol. Obstet. Invest. 64:187–192. doi:10.1159/000106488

Blanton, L. V., M. R. Charbonneau, T. Salih, M. J. Barratt, S. Venkatesh, O. Ilkaveya, S. Subramanian, M. J. Manary, I. Trehan, J. M. Jorgensen, et al. 2016. Gut bacteria that prevent growth impairments transmitted by microbiota from malnourished children. Science 351(6275). doi:10.1126/science.aad3311

Bolger, A. M., M. Lohse, and B. Usadel. 2014. Trimmomatic: a flexible trimmer for Illumina sequence data. Bioinformatics 30:2114–2120. doi:10.1093/bioinformatics/btu170

Charbonneau, M. R., D. O'Donnell, L. V. Blanton, S. M. Totten, J. C. Davis, M. J. Barratt, J. Cheng, J. Guruge, M. Talcott, J. R. Bain, et al. 2016. Sialylated milk oligosaccharides promote microbiota-dependent growth in models of infant undernutrition. Cell 164:859–871. doi:10.1016/j.cell.2016.01.024

Council, N. R. 2012. Nutrient requirements of swine: eleventh revised edition. The National Academies Press, Washington, DC.

Ding, Y. X., and H. Cui. 2017. Integrated analysis of genome-wide DNA methylation and gene expression data provide a regulatory network in intrauterine growth restriction. Life Sci. 179:60–65. doi:10.1016/j.lfs.2017.04.020

Dong, L., X. Zhong, H. Ahmad, W. Li, Y. Wang, L. Zhang, and T. Wang. 2014. Intrauterine growth restriction impairs small intestinal mucosal immunity in neonatal piglets. J. Histochem. Cytochem. 62:510–518. doi:10.1369/0022155414532655

Duffield, J. A., T. Vuocolo, R. Tellam, J. R. McFarlane, K. G. Kauter, B. S. Muhlhausler, and I. C. McMillen. 2009. Intrauterine growth restriction and the sex specific programming of leptin and peroxisome proliferator-activated receptor gamma (PPARgamma) mRNA expression in visceral fat in the lamb. Pediatr. Res. 66:59–65. doi:10.1203/PDR.0b013e3181a7c121

Hanson, R. W., and Y. M. Patel. 1994. Phosphoenolpyruvate carboxykinase (GTP): the gene and the enzyme. Adv. Enzymol. Relat. Areas Mol. Biol. 69:203–281.

Hevener, A. L., W. He, Y. Barak, J. Le, G. Bandyopadhyay, P. Olson, J. Wilkes, R. M. Evans, and J. Olefsky. 2003. Muscle-specific Pparg deletion causes insulin resistance. Nat. Med. 9:1491–1497. doi:10.1038/nm956

Holub, M., D. A. Lawrence, N. Andersen, A. Davidová, O. Beran, V. Marešová, and P. Chalupa. 2013. Cytokines and chemokines as biomarkers of community-acquired bacterial infection. Mediators Inflamm. 2013:190145. doi:10.1155/2013/190145

Hracsko, Z., H. Orvos, Z. Novak, A. Pal, and I. S. Varga. 2008. Evaluation of oxidative stress markers in neonates with intra-uterine growth retardation. Redox Rep. 13:11–16. doi:10.1179/135100008X259097

Hu, Y., L. Hu, D. Gong, H. Lu, Y. Xuan, R. Wang, Wu, D. Chen, K. Zhang, F. Gao, et al. 2018. Genome-wide DNA methylation analysis in jejunum of *Sus scrofa* with intrauterine growth restriction. Mol. Genet. Genomics 293:807–818. doi:10.1007/s00438-018-1422-9

Iwata, F., T. Joh, F. Ueda, Y. Yokoyama, and M. Itoh. 1998. Role of gap junctions in inhibiting ischemia-reperfusion injury of rat gastric mucosa. Am. J. Physiol. 275:G883–G888. doi:10.1152/ajpgi.1998.275.5.G883

Jang, J. H., H. W. Shin, J. M. Lee, H. W. Lee, E. C. Kim, and S. H. Park. 2015. An overview of pathogen recognition receptors for innate immunity in dental pulp. Mediators Inflamm. 2015:794143. doi:10.1155/2015/794143

Jones, J. R., C. Barrick, K. A. Kim, J. Lindner, B. Blondeau, Y. Fujimoto, M. Shiota, R. A. Kesterson, B. B. Kahn, and M. A. Magnuson. 2005. Deletion of PPARgamma in adipose tissues of mice protects against high fat diet-induced obesity and insulin resistance. Proc. Natl. Acad. Sci. USA 102:6207–6212. doi:10.1073/pnas.0306743102

Joss-Moore, L. A., Y. Wang, M. L. Baack, J. Yao, A. W. Norris, X. Yu, C. W. Callaway, R. A. McKnight, K. H. Albertine, and R. H. Lane. 2010. IUGR decreases PPARγ and SETD8 expression in neonatal rat lung and these effects are ameliorated by maternal DHA supplementation. Early Hum. Dev. 86:785–791. doi:10.1016/j.earlhumdev.2010.08.026

Kim, D., B. Langmead, and S. L. Salzberg. 2015. HISAT: a fast spliced aligner with low memory requirements. Nat. Methods 12:357–360. doi:10.1038/nmeth.3317

Kumar, N. M., and N. B. Gilula. 1996. The gap junction communication channel. Cell 84:381–388. doi:10.1016/s0092-8674(00)81282-9

Lehrke, M., and M. A. Lazar. 2005. The many faces of PPARgamma. Cell 123:993–999. doi:10.1016/j.cell.2005.11.026

Lin, G., C. Liu, C. Feng, Z. Fan, Z. Dai, C. Lai, Z. Li, G. Wu, and J. Wang. 2012. Metabolomic analysis reveals differences in umbilical vein plasma metabolites between normal and growth-restricted fetal pigs during late gestation. J. Nutr. 142:990–998. doi:10.3945/jn.111.153411

Liu, J., J. He, Y. Yang, J. Yu, X. Mao, B. Yu, and D. Chen. 2014. Effects of intrauterine growth retardation and postnatal high-fat diet on hepatic inflammatory response in pigs. Arch. Anim. Nutr. 68:111–125. doi:10.1080/1745039X.2014.897532

Liu, C., G. Lin, X. Wang, T. Wang, G. Wu, D. Li, and J. Wang. 2013. Intrauterine growth restriction alters the hepatic proteome in fetal pigs. J. Nutr. Biochem. 24:954–959. doi:10.1016/j.jnutbio.2012.06.016

Livak, K. J., and T. D. Schmittgen. 2001. Analysis of relative gene expression data using real-time quantitative PCR

and the 2(-delta delta C(T)) method. Methods 25:402–408. doi:10.1006/meth.2001.1262

Love, M. I., W. Huber, and S. Anders. 2014. Moderated estimation of fold change and dispersion for RNA-seq data with DESeq2. Genome Biol. 15:550. doi:10.1186/s13059-014-0550-8

Lugrin, J., N. Rosenblatt-Velin, R. Parapanov, and L. Liaudet. 2014. The role of oxidative stress during inflammatory processes. Biol. Chem. 395:203–230. doi:10.1515/hsz-2013-0241

Luo, Z., W. Luo, S. Li, S. Zhao, T. Sho, X. Xu, J. Zhang, W. Xu, and J. Xu. 2018. Reactive oxygen species mediated placental oxidative stress, mitochondrial content, and cell cycle progression through mitogen-activated protein kinases in intrauterine growth restricted pigs. Reprod. Biol. 18:422–431. doi:10.1016/j.repbio.2018.09.002

Mach, N., M. Berri, D. Esquerré, C. Chevaleyre, G. Lemonnier, Y. Billon, P. Lepage, I. P. Oswald, J. Doré, C. Rogel-Gaillard, et al. 2014. Extensive expression differences along porcine small intestine evidenced by transcriptome sequencing. PLoS One 9:e88515. doi:10.1371/journal.pone.0088515

Matsusue, K., M. Haluzik, G. Lambert, S. H. Yim, O. Gavrilova, J. M. Ward, B. Brewer, Jr, M. L. Reitman, and F. J. Gonzalez. 2003. Liver-specific disruption of PPARgamma in leptin-deficient mice improves fatty liver but aggravates diabetic phenotypes. J. Clin. Invest. 111:737–747. doi:10.1172/JCI17223

McLamb, B. L., A. J. Gibson, E. L. Overman, C. Stahl, and A. J. Moeser. 2013. Early weaning stress in pigs impairs innate mucosal immune responses to enterotoxigenic *E. coli* challenge and exacerbates intestinal injury and clinical disease. PLoS One 8:e59838. doi:10.1371/journal.pone.0059838

Moeser, A. J., C. V. Klok, K. A. Ryan, J. G. Wooten, D. Little, V. L. Cook, and A. T. Blikslager. 2007. Stress signaling pathways activated by weaning mediate intestinal dysfunction in the pig. Am. J. Physiol. Gastrointest. Liver Physiol. 292:G173–G181. doi:10.1152/ajpgi.00197.2006

Nebert, D. W., and D. W. Russell. 2002. Clinical importance of the cytochromes P450. Lancet 360:1155–1162. doi:10.1016/S0140-6736(02)11203-7

Neurath, M. F., and S. Finotto. 2011. IL-6 signaling in autoimmunity, chronic inflammation and inflammation-associated cancer. Cytokine Growth Factor Rev. 22:83–89. doi:10.1016/j.cytogfr.2011.02.003

Palomino, D. C., and L. C. Marti. 2015. Chemokines and immunity. Einstein (Sao Paulo) 13:469–473. doi:10.1590/S1679-45082015RB3438

Penhoat, A., L. Fayard, A. Stefanutti, G. Mithieux, and F. Rajas. 2014. Intestinal gluconeogenesis is crucial to maintain a physiological fasting glycemia in the absence of hepatic glucose production in mice. Metabolism 63:104–111. doi:10.1016/j.metabol.2013.09.005

Pluske, J. R., D. J. Hampson, and I. H. Williams. 1997. Factors influencing the structure and function of the small intestine in the weaned pig: a review. Livest. Prod. Sci. 51:215–236. doi:10.1016/S0301-6226(97)00057-2

Ren, W., J. Yin, H. Xiao, S. Chen, G. Liu, B. Tan, N. Li, Y. Peng, T. Li, B. Zeng, et al. 2016. Intestinal microbiota-derived GABA mediates interleukin-17 expression during enterotoxigenic *Escherichia coli* infection. Front. Immunol. 7:685. doi:10.3389/fimmu.2016.00685

Soo, J. Y., M. D. Wiese, M. J. Berry, I. C. McMillen, and J. L. Morrison. 2018. Intrauterine growth restriction may reduce hepatic drug metabolism in the early neonatal period. Pharmacol. Res. 134:68–78. doi:10.1016/j.phrs.2018.06.003

Su, W., W. Xu, H. Zhang, Z. Ying, L. Zhou, L. Zhang, and T. Wang. 2017. Effects of dietary leucine supplementation on the hepatic mitochondrial biogenesis and energy metabolism in normal birth weight and intrauterine growth-retarded weanling piglets. Nutr. Res. Pract. 11:121–129. doi:10.4162/nrp.2017.11.2.121

Subramanian, S., S. Huq, T. Yatsunenko, R. Haque, M. Mahfuz, M. A. Alam, A. Benezra, J. DeStefano, M. F. Meier, B. D. Muegge, et al. 2014. Persistent gut microbiota immaturity in malnourished Bangladeshi children. Nature 510:417–421. doi:10.1038/nature13421

Tagawa, T., H. Nishimura, T. Yajima, H. Hara, K. Kishihara, G. Matsuzaki, I. Yoshino, Y. Maehara, and Y. Yoshikai. 2004. V 1+ T cells producing CC chemokines may bridge a gap between neutrophils and macrophages in innate immunity during *Escherichia coli* infection in mice. J. Immunol. 173:5156–5164. doi:10.4049/jimmunol.173.8.5156

Tan, B., X. G. Li, X. Kong, R. Huang, Z. Ruan, K. Yao, Z. Deng, M. Xie, I. Shinzato, Y. Yin, et al. 2009. Dietary L-arginine supplementation enhances the immune status in early-weaned piglets. Amino Acids 37:323–331. doi:10.1007/s00726-008-0155-1

Trapnell, C., A. Roberts, L. Goff, G. Pertea, D. Kim, D. R. Kelley, H. Pimentel, S. L. Salzberg, J. L. Rinn, and L. Pachter. 2012. Differential gene and transcript expression analysis of RNA-seq experiments with TopHat and Cufflinks. Nat. Protoc. 7:562–578. doi:10.1038/nprot.2012.016

Wang, Z., M. Gerstein, and M. Snyder. 2009. RNA-seq: a revolutionary tool for transcriptomics. Nat. Rev. Genet. 10:57–63. doi:10.1038/nrg2484

Wang, X., G. Lin, C. Liu, C. Feng, H. Zhou, T. Wang, D. Li, G. Wu, and J. Wang. 2014. Temporal proteomic analysis reveals defects in small-intestinal development of porcine fetuses with intrauterine growth restriction. J. Nutr. Biochem. 25:785–795. doi:10.1016/j.jnutbio.2014.03.008

Wang, X., W. Wu, G. Lin, D. Li, G. Wu, and J. Wang. 2010. Temporal proteomic analysis reveals continuous impairment of intestinal development in neonatal piglets with intrauterine growth restriction. J. Proteome Res. 9:924–935. doi:10.1021/pr900747d

Wang, J., L. Zeng, B. Tan, G. Li, B. Huang, X. Xiong, F. Li, X. Kong, G. Liu, and Y. Yin. 2016. Developmental changes in intercellular junctions and Kv channels in the intestine of piglets during the suckling and post-weaning periods. J. Anim. Sci. Biotechnol. 7:4. doi:10.1186/s40104-016-0063-2

Wijtten, P. J., J. van der Meulen, and M. W. Verstegen. 2011. Intestinal barrier function and absorption in pigs after weaning: a review. Br. J. Nutr. 105:967–981. doi:10.1017/S0007114510005660

Winterhager, E., and A. Gellhaus. 2017. Transplacental nutrient transport mechanisms of intrauterine growth restriction in rodent models and humans. Front. Physiol. 8:951. doi:10.3389/fphys.2017.00951

Wu, G., F. W. Bazer, J. M. Wallace, and T. E. Spencer. 2006. Board-invited review: intrauterine growth retardation:

implications for the animal sciences. J. Anim. Sci. 84:2316–2337. doi:10.2527/jas.2006-156

Wu, L., W. Wang, K. Yao, T. Zhou, J. Yin, T. Li, L. Yang, L. He, X. Yang, H. Zhang, et al. 2013. Effects of dietary arginine and glutamine on alleviating the impairment induced by deoxynivalenol stress and immune relevant cytokines in growing pigs. PLoS One 8:e69502. doi:10.1371/journal.pone.0069502

Xu, R. J., F. Wang, and S. H. Zhang. 2000. Postnatal adaptation of the gastrointestinal tract in neonatal pigs: a possible role of milk-borne growth factors. Livest. Prod. Sci. 66:95–107. doi:10.1016/S0301-6226(00)00217-7

Yang, H. S., F. Wu, L. N. Long, T. J. Li, X. Xiong, P. Liao, H. N. Liu, and Y. L. Yin. 2016. Effects of yeast products on the intestinal morphology, barrier function, cytokine expression, and antioxidant system of weaned piglets. J. Zhejiang Univ. Sci. B 17:752–762. doi:10.1631/jzus.B1500192

Yen, D., J. Cheung, H. Scheerens, F. Poulet, T. McClanahan, B. McKenzie, M. A. Kleinschek, A. Owyang, J. Mattson, W. Blumenschein, et al. 2006. IL-23 is essential for T cell-mediated colitis and promotes inflammation via IL-17 and IL-6. J. Clin. Invest. 116:1310–1316. doi:10.1172/JCI21404

Zhu, Y., W. Wang, T. Yuan, L. Fu, L. Zhou, G. Lin, S. Zhao, H. Zhou, G. Wu, and J. Wang. 2017. Microrna-29a mediates the impairment of intestinal epithelial integrity induced by intrauterine growth restriction in pig. Am. J. Physiol. Gastrointest. Liver Physiol. 312:G434–G442. doi:10.1152/ajpgi.00020.2017